Heterogeneity within an HSV-1 Wild-Type Strain and Its Importance in Pathogenesis

(42934)

ANN MONTGOMERY[1] AND YSOLINA CENTIFANTO[2]
Department of Ophthalmology, Tulane University School of Medicine, New Orleans, Louisiana 70112

Abstract. **A herpes simplex virus-type 1 low passage, clinical eye isolate, E-43 at P2, was compared with its variant progeny, SLi-43 at P8, in terms of ocular disease, cytopathic effects, and genomic variation. In New Zealand White (NZW) rabbits, E-43 produced mild epithelial defects and punctate lesions with full recovery by Day 10 postinfection (pi). SLi-43 caused dendritic lesions, progressing to geographic ulceration and death from herpes simplex virus encephalitis in 10 days postinfection. In RK, Hep-2, and Vero cells, E-43 displayed the *syn*$^+$ phenotype (aggregation and cell rounding); SLi-43 showed the *syn* phenotype (syncytium formation). DNA digestion profiles of E-43, SLi-43, and isolates from the brains of infected animals showed that the genomic differences map within the terminal repeat of the unique long segment and the internal joint region, specifically in bands B, E, N, and S (*Bam* HI) and bands M and N (*Hind* III). Analysis of the DNA of virus recovered from the brain stem of SLi-43-infected, encephalitic rabbits demonstrated that an *in vivo* selection for neurotropic virions had taken place. Plaque purification of 20 clones from the original E-43 strain showed that one of 20 was the *syn* phenotype, indicating that the SLi-43 variant was present in the original E-43 isolate and did not develop *de novo* by rapid mutation. The parent-progeny relationship between E-43 and SLi-43 forms an ideal model in which to compare differences in pathogenicity at the genomic level, and underscores the importance of heterogeneity within a single herpes simplex virus-type 1 wild-type population in terms of variations in ocular disease.** [P.S.E.B.M. 1989, Vol 191]

Ocular infections with the wild-type herpes simplex virus-type 1 (HSV-1) in the rabbit are characterized primarily by dendritic ulcers in the epithelial layer of the cornea (1–3). In some infections this leads to a severe necrotizing stromal keratitis and corneal vascularization (4–7), but rarely to encephalitis (8, 9).

Differences in ocular herpetic diseases have been ascribed to variations in the genome of HSV-1 strains (10). The morphology of ocular lesions and the type and severity of disease are genetically determined by the virus strain. Recombinant DNA and DNA fingerprinting has shown a positive correlation between strains and their characteristic ocular herpetic disease patterns (11). Therefore, we chose to compare strains that produce mild eye diseases with strains that produce fatal encephalitis, the most severe form of HSV-1 disease.

We know that the herpes virus remains latent in the trigeminal ganglia following primary ocular infection (12–14), but we are not certain how the virus enters the central nervous system in herpes simplex encephalitis. Two possibilities are via the olfactory route and via the trigeminal ganglia (15–17). It is unclear whether the acute encephalitis caused by HSV-1 in humans represents primary infection, reinfection, or reactivation of the latent virus. Although the exact basis for the pathogenicity of herpes simplex encephalitis is obscure, some HSV-1 strains have been demonstrated as neurotropic in animal models while other strains have not (18). Differentiating neurotropic strains from non-neurotropic strains or recurrent from nonrecurrent strains is difficult because of the complexity of the HSV genome and its relatively large size (19). Comparisons are more accurately made between closely related isolates that differ in only one aspect of their disease pattern.

[1] Current address: IMREG, Inc., New Orleans, Louisiana.

[2] All correspondences and reprint requests should be sent to Ysolina Centifanto, Department of Ophthalmology, Tulane University School of Medicine, 1430 Tulane Ave., New Orleans, Louisiana 70112.

Received September 7, 1988. [P.S.E.B.M. 1989, Vol 191]
Accepted March 15, 1989.

0037-9727/89/1914-0362$2.00/0

We have characterized an epithelial disease-producing virus, HSV-1 (E-43), and its progeny, HSV-1 (SLi-43), which causes fatal encephalitis in rabbits. We expected the nucleotide sequence of the parents and progeny to be sufficiently similar, such that differences in DNA sequences might be related to the differences in CPE between parent and progeny as well as to the neurotropic nature of the encephalitis-causing variant.

Specifically, we examined cytopathic effects, plaque morphology in different cell lines, the ocular disease pattern produced by these isolates, and genomic differences as determined by restriction endonuclease mapping. From the neurotropic strains we also sought to determine whether HSV-1 (SLi-43) arose *de novo*, through tissue culture passage of the E-43 isolate, or resulted from an *in vitro* or an *in vivo* selection of a variant already present in the heterogeneous parental stock.

Materials and Methods

Cells and Viruses. RK-13 and Hep-2 cells (Whittaker M. A. Bioproducts, Walkersville, MD) were grown in minimal essential medium supplemented with 10% fetal calf serum, 1% glutamine, sodium bicarbonate, and antibiotics. Vero cells grown in minimal essential medium (Eagle's), supplemented with 10% fetal calf serum, were used for the DNA work.

HSV-1 (E-43), a low passage (P2) clinical isolate, HSV-1 (SLi-43), a variant derived from E-43 with an increased mortality in rabbits, HSV-1 (F), a prototype strain, and HSV-1 (MP), which produces fatal encephalitis in rabbits, were the HSV-1 strains used in this study. The SLi-43 strain was initially passed in RK-13 cells and then in Hep-2 cells (P8).

Ocular Disease Model. New Zealand White rabbits (3–5 kg body wt) were used as the ocular disease model (20). Two drops of Ophthaine were instilled for topical anesthesia, and the corneas were lightly scarified. To infect each eye, 50 μl of a virus suspension (10^5 plaque-forming units) were dropped onto the surface and the lids rubbed twice over the cornea. All eyes were examined by the slit lamp on Day 3 postinfection (PI) to confirm herpetic infection and three times weekly for 3 weeks to document the disease pattern. Three rabbits were assigned per virus strain. During the first 10 days, eye readings were done in a masked fashion. Animals infected with a particular strain were identity coded so that we could accurately record the disease patterns in an unbiased way.

Virus Recovery from Trigeminal Ganglia. The trigeminal ganglia were excised and washed with phosphate-buffered saline containing 10% gentamicin. The tissue was minced aseptically and subjected to collagenase and trypsin digestion as described by Nesburn *et al.* (21). The entire sample of digested tissue was seeded onto young confluent RK-13 monolayer cultures. These were incubated at 37°C for 2–4 weeks, with several changes of maintenance medium. All positive cultures of the same ganglia were pooled, dispensed into small vials, and stored at −70°C for later use.

Viral DNA Purification. Confluent monolayers of Vero cells were infected with the viral isolates at a multiplicity of approximately 1 plaque-forming unit/cell and incubated at 37°C in phosphate-free medium containing 100 μCi of [^{32}P]orthophosphate (New England Nuclear, Boston, MA). At 24–36 hr PI, the medium was decanted and cells were disrupted with 0.5 ml of NP-40 in 1 mM EDTA/10 mM Tris buffer (pH 7.8). The suspension was kept for 5 min at room temperature, then aspirated 10 times with a Pasteur pipette and transferred to 1.5-ml Eppendorf centrifuge tubes. The cell suspension was then spun for 5 min in a microfuge to pellet the nuclei. The nuclear debris was discarded. Sodium dodecyl sulfate was added to the supernatant for a final concentration of 0.5%. The cytoplasmic RNA was degraded by treatment with 50 μg of RNase A for 30 min at 37°C, and 250 μg of Proteinase K (Boehringer Mannheim Biochemical, Indianapolis, IN) were added to each culture. The suspension was incubated for 1 hr at 56°C. The resulting lysate was extracted twice with phenol, then three times with ether to remove the residual phenol. Twenty-five micrograms of sonicated salmon sperm DNA (Sigma, St. Louis, MO) were added as a carrier, and the total DNA was removed by overnight precipitation with ethanol at −20°C.

Endonuclease Digestion and Electrophoresis. Viral DNA was digested with restriction endonuclease enzymes (New England Biolabs, Beverly, MA) in a 50-μl reaction mixture at 37°C according to the manufacturer's instructions. As an internal control for enzyme activity, λ phage DNA was cleaved and *Hin*d III fragments were used as sizing markers. Restriction enzyme digestions were subjected to electrophoresis in a 0.8% agarose submerged horizontal gel slab at 2 V/cm. The stock loading solution contained 0.05% bromophenol blue, 0.05% xylene cyanole, and 50% sucrose in 0.01 *M* Tris (pH 7.8). Electrophoresis was carried out on a submergible gel apparatus (Bethesda Research Laboratories, Bethesda, MD). The running buffer, containing 5 mM sodium acetate and 1 mM EDTA in 40 mM Tris (pH 7.8), was circulated continuously. The gels were run at a constant voltage of 40 V for 18–20 hr. Following electrophoresis, the gels were stained in a 1 μg/ml ethidium bromide bath at 4°C for 1 hr, visualized under UV light, photographed, and dried. Autoradiography was performed with DuPont Chronex Lightning-Plus intensifying screens with Kodak XAR-5 x-ray film at −70°C for 1–4 days.

Experimental Design. The parent strain E-43 (P2), its variant SLi-43 grown in Hep-2 cells, and three successive passes of this variant made in Vero cells labeled SLi-43 (P8), SLi-43 (P9), and SLi-43 (P10) are the five strains used for this project. These virus stocks

were used to inoculate the rabbits and then the virus present in the brain stem and trigeminal ganglia was recovered from the infected animals. The parent and progeny viruses were characterized as to corneal disease pattern, mortality in rabbits, *in vitro* cytopathogenic effects, and viral DNA profiles.

Results

Characterization of the Parent Strains. *Ocular disease.* The disease produced by HSV-1 (E-43) was characterized by punctate staining and a few dendritic ulcers involving less than one fourth of the corneal surface. The disease cleared by Day 10 PI with no scarring or mortality. Infection with the HSV-1 (SLi-43) produced thick dendritic ulcers which coalesced to form large geographic defects. Although the ocular disease did not progress to stromal keratitis, these animals became lethargic and died of encephalitis within 7–19 days PI.

Cytopathic effects. The plaque morphology and cytopathic effects of the parental strains were determined on Vero, Hep-2, and RK-13 cell cultures. HSV-1 (E-43) caused classical rounding and aggregation of the cells in all cell cultures. SLi-43 consistently yielded polykaryocyte formation, which was more pronounced in Vero cells (Fig. 1).

The rounding and aggregation of infected cells is the classical most common type of cytopathic effect caused by HSV wild-type strains. Polykaryocyte characterized by giant cells containing many nuclei is more common in laboratory strains and is rarely found in fresh isolates.

Viral DNA analysis. Restriction endonuclease analysis of viral DNA in HSV-1 (E-43) was performed using *Bam* HI. The HSV-1 (MP) strain was included in the E-43 analysis to rule out possible contamination of the HSV-1 (SLi-43) virus stock, as this strain causes syncytial formation in tissue cultures as well as encephalitis in rabbits. Each virus isolate gave a distinct digestion profile permitting the differentiation of one virus from another and ruling out contamination with the MP strain (Fig. 2).

In vivo passage. Several experiments were designed to determine whether accumulation of variants within the virus stock was responsible for the biologic differences between the HSV-1 (E-43) parent and successive passages of the HSV-1 (SLi-43) variant. For example, the HSV-1 (SLi-43 P8) virus was passaged *in vitro* in Vero cells to obtain a working virus stock of P9. The cytopathic effects of this passage were characterized and the HSV-1 (SLi-43 P9) was used to infect several rabbits. The ocular disease was graded, mortality was recorded, and virus was isolated from both the ganglia and the brain stem of each rabbit. As a diminished presence of syncytial formation was observed when generating the *in vitro* HSV-1 (SLi-43 P9), this passage was in turn used to generate a P10 *in vitro* passage to determine whether a dilution of the *syn* phenotype was occurring in the SLi-43 stock. Both P9 and P10 passages showed a decrease in syncytial formation (Table I).

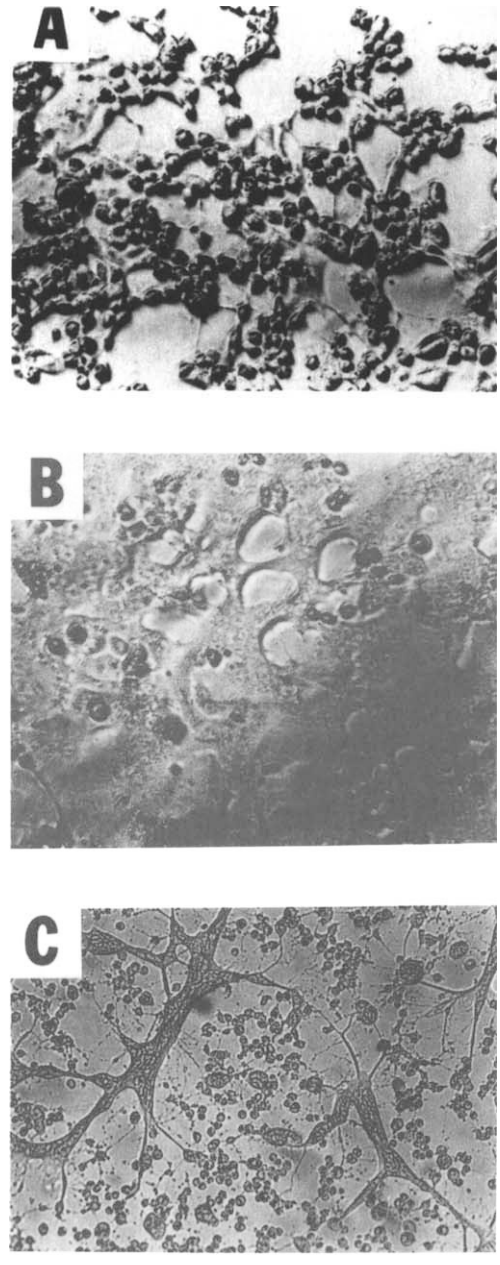

Figure 1. Cytopathogenic effects observed in Vero cell cultures infected with HSV-1 strains. (A) Cell culture infected with HSV-1 (E-43) exhibiting the *syn*$^+$ phenotype that consists of aggregation and rounding of cells. (B) HSV-1 (SLi-43 P8)-infected cells exhibiting extensive syncytial formation characteristic of the *syn* phenotype. (C) HSV-1 (SLi-43 P10)-infected cells exhibiting both syncytial formation (*syn* phenotype) and rounding of cells (*syn*$^+$ phenotype).

To determine if a decreased *syn* phenotype correlated with a decline in morbidity and mortality, the three successive passages of HSV-1 (SLi-43) were used to infect three more rabbits. The disease course was recorded, and virus was recovered from the trigeminal ganglia and/or the brain stem of all encephalitic rabbits (Table II). The rabbits infected with the HSV-1 (SLi-43 P10) developed ocular disease similar to that of the

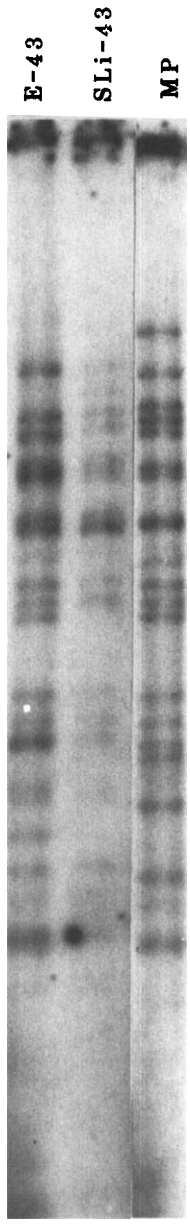

Figure 2. *Bam* HI restriction endonuclease analysis of viral DNA from HSV-1 (E-43), HSV-1 (SLi-43), and HSV-1 (MP). Each strain has its unique and distinct DNA profile.

parent HSV-1 (SLi-43)-infected rabbits. However, unlike the rabbits infected with SLi-43 P8 and P9 that died as early as Day 7 PI, rabbits infected with HSV-1 (SLi-43 P10) died at 16–19 days PI. The extended time of life of the rabbits infected with HSV-1 (SLi-43 P10) correlated with diminished syncytial formation noted in this virus stock.

The variations on the *syn* phenotype of the several passages of HSV-1 (SLi-43) are shown in Figure 1. Infected cultures of the parent HSV-1 (E-43) exhibit the *syn*$^+$ phenotype with its characteristic rounding of the cells. The HSV-1 (SLi-43 P8) shows extensive syncytial formation, which is characteristic of the *syn* phenotype. In contrast, cell cultures infected with the HSV-1 (SLi-43 P10) show a mixture of the two phenotypes,

Table I. *In Vitro* Cytopathogenic Effect of the Different HSV Inoculum in Vero Cells

Virus	
HSV-1 (E-43 p1)	*syn*$^+$ phenotype; 100% aggregation
HSV-1 (SLi-43 P8)	*syn* phenotype; 90% fusion/ 10% aggregation
HSV-1 (SLi-43 P9)	*syn* phenotype; 70% fusion/ 30% aggregation
HSV-1 (SLi-43 P10)	*syn*$^+$ phenotype; 30% fusion/ 70% aggregation

[a] syn$^+$ denotes cell rounding and aggregation of infected cells. syn denotes syncytial formation of infected cells.

Table II. *In Vivo* Morbidity and Mortality in Rabbits Infected with HSV-1 (SLi-43) Variants[a]

Inoculum	Rabbit	Viral recovery[b] (trigeminal ganglia and/or brain stem)	Mortality (days PI)
SLi-43 P8	3710	+	7
SLi-43 P8	3711	+	—[c]
SLi-43 P9	3865	+	8
SLi-43 P9	3943	+	8
SLi-43 P9	3872	+	10
SLi-43 P10	3185	+	16
SLi-43 P10	3527	+	19
SLi-43 P10	3528		No

[a] New Zealand White rabbits were infected with 100 μl of the different inocula of the HSV-1 strains as described in Materials and Methods. Animals were examined daily and the mortality was recorded.
[b] HSV recovery by co-cultivation of processed trigeminal ganglia or brain stem was not performed on animals that died overnight or on weekends. In these animals, tissue samples of both organs were minced and directly plated onto monolayer cell cultures of Vero cells.
[c] This rabbit had severe encephalitis and was sacrificed at 7 days PI.

the extensive syncytial formation seen in earlier passages has diminished considerably, and the majority of the infected cells show a *syn*$^+$ phenotype.

Comparative DNA analysis. Restriction endonuclease digestion was used to analyze the DNA of the various strains, as well as DNA from the viruses isolated from the brain stem or trigeminal ganglia of infected animals. To demonstrate possible genomic variations among the strains, the HSV-1 (F) prototype strain was used as an internal standard, thus establishing digestion profile differences in accordance with the published maps of the HSV-1 (F) genome (22).

Figure 3 represents a *Bam* HI digestion profile displaying the band differences among HSV-1 (E-43), HSV-1 (SLi-43 P8), and isolate 3710B, which was recovered from the brain of an animal infected with the HSV-1 (SLi-43 P8). Differences were found in all three viruses. Arrows to the left indicate the differences between digestion profiles of the HSV-1 strains, that is to say differences in bands between the parent HSV-1 (E-43) and its variant HSV-1 (SLi-43) and the virus re-

covered from the brain of an animal infected with HSV-1 (SLi-43). Using published genomic maps of HSV-1 detailing the cleavage sites, locations were assigned for some of the common band changes.

Band differences were further elucidated in Figure 4 which depicts another *Bam* HI DNA digestion profile of HSV-1 (E-43), HSV-1 (SLi-43 P8 and P9), and two isolates obtained from the brain of animals infected with HSV-1 (SLi-43 P8) and HSV-1 (SLi-43 P9), and also another isolate 3185B, which was recovered from a rabbit infected with HSV-1 (SLi-43 P10). No differences were observed between the HSV-1 (SLi-43) and passages 8 and 9 regarding banding profiles and total DNA recovered. The only observed difference between them was the relative intensity of band B. This observation is important in that it suggests a greater amount of heterogeneity within the viruses with regard to the presence or absence of cleavage sites for band B, especially in view of the fact that the original parent (E-43) lacks band B. The DNA profile of isolate 3185B from a rabbit infected with HSV-1 (SLi-43 P10) shows a profile closer to the original parent HSV-1 (E-43), as it lacks band B. The differences between this isolate and the parent only occur in bands L, M, and N. We note

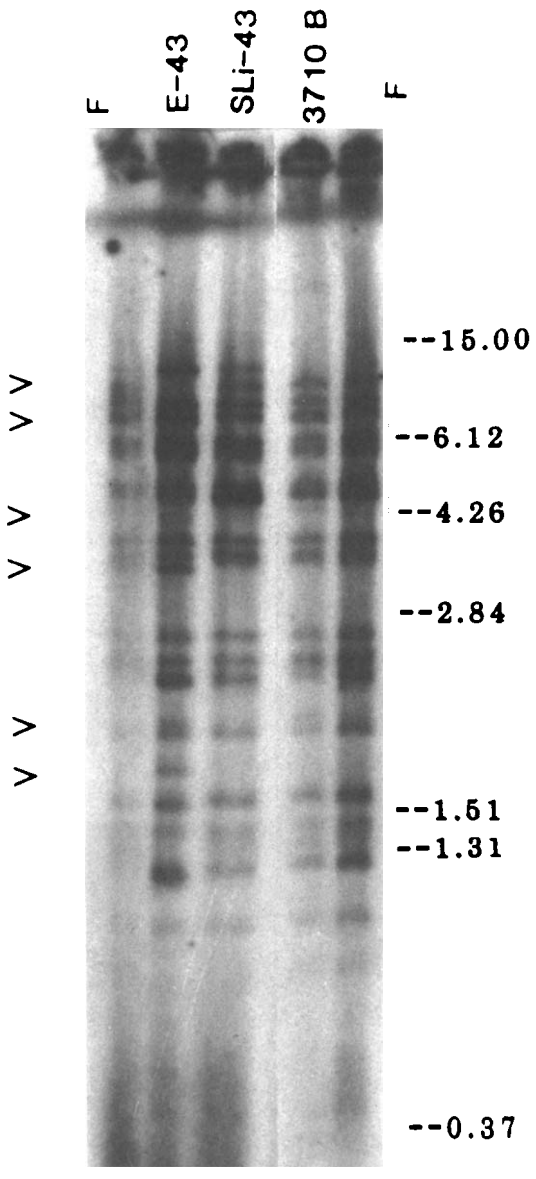

Figure 3. Viral DNA was digested with *Bam* HI restriction endonuclease enzyme. Unlabeled λ DNA cut with *Hind III* was used as molecular weight marker. Molecular weight values for the resulting 7 λ band fragments appear on the right side of this photograph. These values are in kilodaltons ($\times 10^6$). HSV-1 (F) appearing in Lanes 1 and 5 serve as internal standards with which to compare these fragments against published HSV-1 (F) genomic maps. Arrows to the left indicate differences observed between the DNA digestion profiles of the viral isolates.

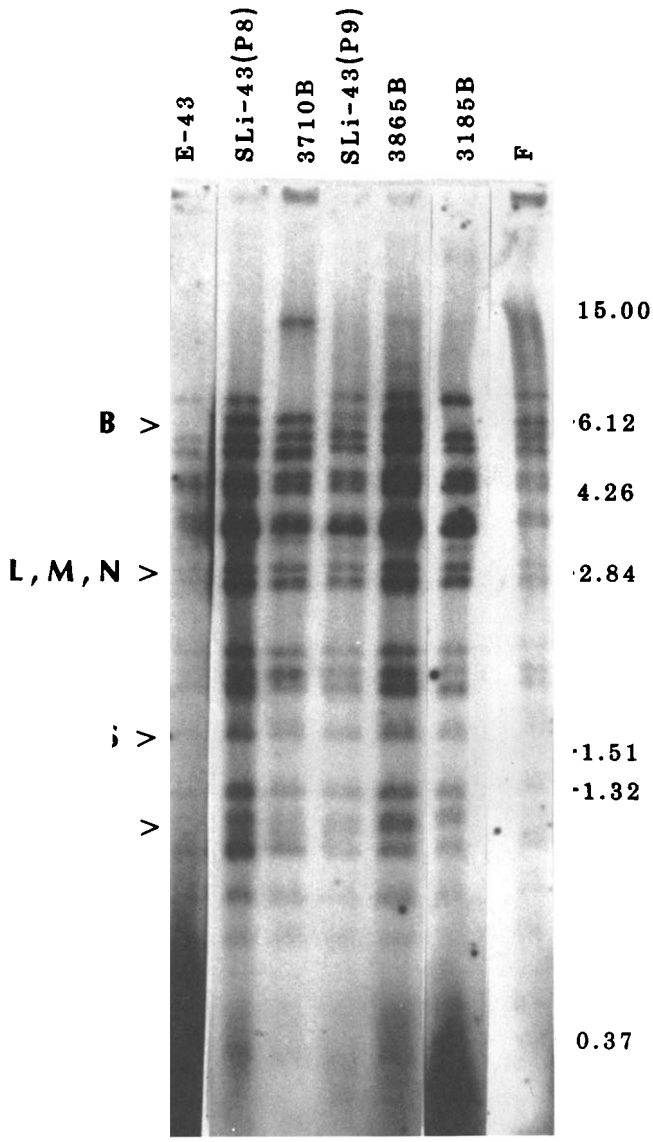

Figure 4. Viral DNA from the various isolates was digested with *Bam* HI restriction endonuclease enzyme. Unlabeled λ DNA cut with *Hind III* was used as a molecular weight marker. Molecular weight values for the resulting λ band fragments appear at the right and are in kilodaltons ($\times 10^6$). SLi-43 (P8) was used to infect Rabbit 3710, SLi-43 (P9) was used to infect Rabbit 3865, and Rabbit 3185 was infected with SLi-43 (P10). Arrows to the left indicate differences observed between the DNA digestion profiles of the viral isolates.

HSV-1 (E-43) displays a triplet for bands L, M, and N, while the isolate 3185B shows a doublet with bands M and N congregating as one thick band on the autoradiograph. This observation of bands M and N appearing as a single fused band in a *Bam* HI digestion profile has been observed in all viruses recovered from the brain of encephalitic animals (Fig. 4). Both the inoculating strains, HSV-1 (SLi-43 P8 and SLi-43 P9), appear to have the same doublet with the fused M and N bands as does their respective brain isolates, 3710B and 3865B. In this manner, they do differ from the parental E-43 which shows a triplet, i.e., individual L, M, and N bands (Figs. 3 and 4). Bands designated M and N are located within the short terminal repeats found in the joint region of the HSV-1 genome in the prototype orientation, as seen in HSV-1 published genomic maps (23).

There are two other band differences within these isolates: (1) Band S with an approximate M_r of 1.94 million kDa and (2) the last arrow of a band absent in E-43 but present in the other strains. The nomenclature for this band could not be accurately determined from the published HSV-1 genomic maps.

Restriction endonuclease digestion was performed in another experiment using the *Hind* III enzyme (Fig. 5). Because of the relatively large DNA fragments generated with this enzyme, only the smaller fragments in the M_r range of 1–7 million kDa are clearly visible using a 0.8% agarose gel concentration.

The brain isolates shown here are 3710, which was infected with HSV-1 (SLi-43 P8), 3865B and 3872B, which were infected with HSV-1 (SLi-43 P9), and 3185B, which was infected with HSV-1 (SLi-43 P10). The DNA fragments of interest in this autoradiograph are designated bands M, N, and O having M_r of 4.7, 3.2, and 2.0 million kDa, respectively (Fig. 5). While bands M and N are clearly visible in the HSV-1 (E-43) lane, they are clearly absent in all four viral brain isolates (3710B, 3865B, 3872B, and 3185B). In addition, HSV-1 (SLi-43 P8 and P9) exhibits a faint N fragment, indicating heterogeneity of its DNA or a lower copy number of this fragment. The O fragment is absent in the parent E-43, present in both HSV-1 SLi-43 P9 and P9, and fainter in the brain isolates.

E-43 plaque purification. Because of the heterogeneity within the HSV-1 (E-43) stock, the *in vitro* passages and the viruses recovered from the infected animals, the original low passage of HSV-1 (E-43 P2) was plated out to determine whether the syncytium producing plaques could be observed. More specifically, we hoped to determine if the HSV-1 (SLi-43) variant displaying the *syn* phenotype was present in the original parent isolate, or if this variant was generated *de novo* during serial passage of the parent HSV-1 (E-43). We found that from 20 separate plaques picked at random, one plaque displayed the syncytium phenotype characteristic of HSV-1 (SLi-43). Our findings support the hypothesis that the syncytium producing variant must have been present in the initial HSV-1 (E-43) virus stock and did not result *de novo* from rapid mutation of the parental HSV-1 (E-43) strain.

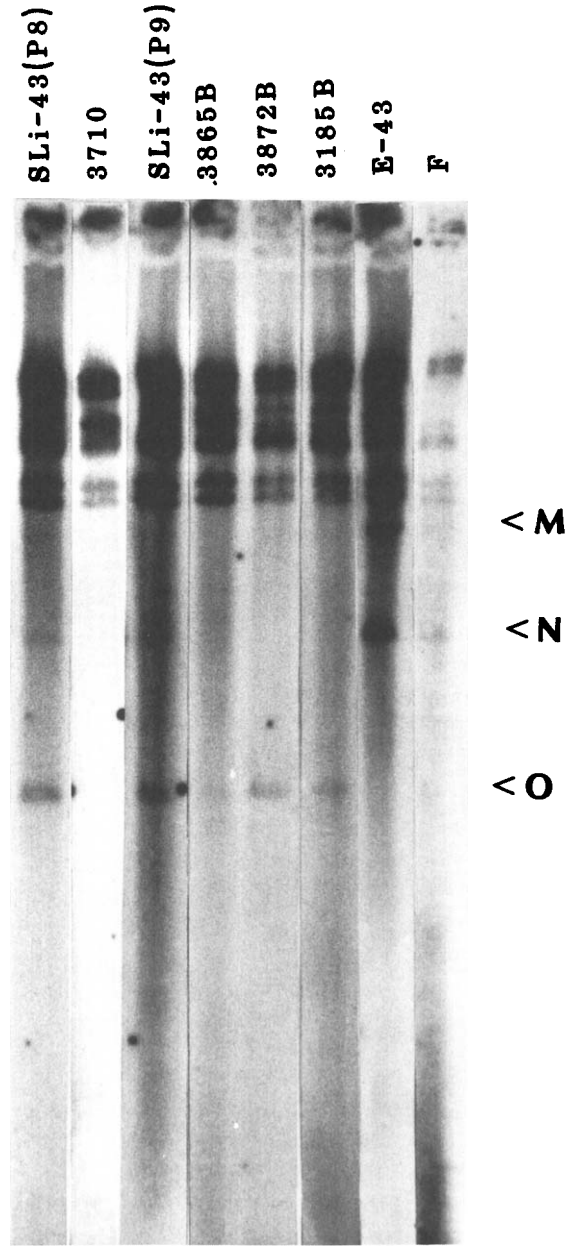

Figure 5. Viral DNA digested with *Hind* III restriction endonuclease. SLi-43 (P8) was used as inoculum to infect Rabbit 3710. SLi-43 (P9) was used as inoculum for Rabbits 3865 and 3872. SLi-43 (P10) was used as inoculum for Rabbit 3185. Note the absence of fragments M and N in all lanes for virus recovered from rabbit brain stem. SLi-43 and SLi-43 (P8) lanes exhibit faint N fragments possibly indicating a lower copy number of this fragment in the digested DNA used as inoculum. The O fragment is absent in the parent E-43, present in SLi-43, and fainter in the brain isolates. The higher molecular weight fragments cannot be accurately identified in this 0.8% agarose cell concentration.

Discussion

The study reports an examination of a variant HSV-1 isolate derived from a low passage (P2) human

eye isolate, HSV-1 (E-43). Indications are that the variant HSV-1 (SLi-43) strain was derived from the original parent virus HSV-1 (E-43), by several *in vitro* passages. Our ability to recover plaques from the parental HSV-1 (E-43) at P2 with the *syn* phenotype suggests that the SLi-43 variant must have been present in the initial parental inocula.

The emergence of a HSV-1 variant with a *syn* phenotype allows the study of genomic rearrangements within a virus population. Because the strains are so closely related, the observed genomic differences would more accurately imply which genomic regions are involved in this pathogenicity.

The E-43 variants differ from the parental strains in important areas: (1) *syn* phenotype or syncytium formation of HSV-1 (SLi-43) contrasted to the syn^+ phenotype characteristic of HSV-1 (E-43); (2) the difference in pathogenicity, i.e., ocular disease and capacity to produce encephalitis; and (3) restriction endonuclease profile differences in DNA among the parental E-43, the variant HSV-1 (SLi-43), and brain isolates recovered from encephalitic rabbits.

Decreased syncytium formation following *in vitro* passage on Vero cells of SLi-43 inoculum suggests a "diluting out" effect of virions responsible for the fusion formation. The decrease in syncytium formation of P8, P9, and P10 correlates with the reduced pathogenicity of the strains (Tables I and II). Successive *in vitro* passages with reduced polykaryocyte formation yielded inocular with reduced capacity to kill rabbits by encephalitis, ranging from death at 7 days, to death at 19 days, to no death at all. This implies a reduction of virions within the stock capable of producing encephalitis in the host.

The DNA profiles of HSV-1 (E-43) and HSV-1 (SLi-43) using *Bam* HI and *Hin*d III restriction endonucleases showed several consistent and reproducible band differences (Figs. 2–4). These findings indicate that the DNA profile differences between the two HSV-1 strains lie within the unique long terminal repeats and the internal joint region of the HSV genome. These regions are known to encode the *syn 1*, *syn 2*, *syn 4*, and *Cr* loci, all of which have been implicated in syncytium formation (24, 25). Because single step revertants are known to occur at high frequency in the terminal and internal repeat regions of the unique short genomic segment and only one wild-type gene is required to regenerate the wild-type phenotype (23), this observation may account for the rapid reversion to syn^+ observed in subsequent SLi-43 passages.

Changes observed in restriction endonuclease profiles have been classified into three types: (1) additions and/or deletions to the terminal repeat sequences and inverted internal repeat sequences; (2) addition and/or deletions to restriction fragments which originate entirely from unique regions of the genome; and (3) the loss and/or gain of restriction endonuclease sites regulating in the generations of new fragments by fusion or additional cleavage (26).

Variations in DNA fragment mobility of viruses isolated from different individuals have been reported. Among these variable fragments, *Bam* HI (N), *Hin*d III (M), and *Hin*d III (N) fragments were found to vary in mobility (27).

The pathogenicity of HSV-1 strains, specifically those that cause encephalitis, may be related to neurotropism. A pathogenic variant, HSV-1 ANG path, was derived from the 15th serial passage in the mouse brain of a plaque-purified clone derived from the originally nonpathogenic HSV-1 ANG strain. Following intraperitoneal infection and death, the variant HSV-1 ANG was recovered from the mouse brain while the HSV-1 parent was not. Both ANG path and ANG parent replicated at the site of primary infection and readily spread to several organs, but only infectious virions of ANG path phenotype appeared in the brain of the infected mice (29). This *in vivo* selection for neurotropic virus occurrence has been reported by several investigators (30–32).

The neurovirulence of HSV-1 strains in the mouse model has also been reported. Becker *et al.* (33) showed that this neurovirulence was genetically determined within the DNA coordinates of 0.762 and 0.787. Similar work by Stevens and colleagues (34, 35) also implicates this region of the DNA. In all of these cases, the differential neurovirulence was determined by the route of injection.

There is no clear evidence to correlate HSV-1 DNA changes with their ability to cause encephalitis in man. The pathogenesis of herpes simplex encephalitis is largely unknown and the incidence of this disease is low. However, in one study of the DNA viruses isolated from encephalitis patients, *Hin*d III (M) and (N) DNA fragments were absent from one isolate and the authors interpreted the absence of these two adjacent fragments to be a result of fusion, yielding a larger fragment obscured by other bands in the higher molecular weight region of the gel (9). This finding is in agreement with the observed loss, in our study, of the M and N fragments in a *Hin*d III digest for all SLi-43 brain isolates tested. The *Hin*d III (N) fragment maps adjacent to the internal repeat of the short component on the HSV-1 prototype genome. This region is also implicated in the HSV-1 ANG genome (29).

The HSV-1 (SLi-43) was not plaque purified in our study, and we found that the relative intensity of the bands on the DNA digestion profile differed between viral inoculum and virus recovered from the rabbit brain. The implication is that there was *in vivo* selection for neurotropic virus. These findings seem to underscore the importance of heterogeneity within a single HSV-1 wild-type strain and its encephalitic potential. Reactivation of a latent virus is thought to be a single event, and reactivation of a neurotropic variant could

lead to encephalitis. Our results are consistent with the theory that encephalitis is due to endogenous reactivation rather than to exogenous infection.

This work was supported in part by a Grant EY06037 from the National Institutes of Health.

1. Nesburn AB, Elliot JM, Leibowitz HM. Spontaneous reactivation of experimental herpes simplex keratitis in rabbits. Arch Ophthalmol **78**:523–529, 1967.
2. Williams LE, Nesburn AB, Kaufman HE. Experimental induction of disciform keratitis. Arch Ophthalmol **73**:112–114, 1965.
3. Kaufman HE, Brown DC, Ellison EM. Recurrent herpes in rabbit and man. Science **156**:1628–1629, 1967.
4. Metcalf JF, Kaufman HE. Herpetic stromal keratitis—Evidence for cell-mediated immunopathogenesis. Am J Ophthalmol **82**:827–834, 1976.
5. Metcalf JF, McNeill JI, Kaufman HE. Experimental disciform edema and necrotizing keratitis in the rabbit. Invest Ophthalmol **15**:979–985, 1976.
6. Centifanto-Fitzgerald YM, Fenger T, Kaufman HE. Virus protein in herpetic keratitis. Exp Eye Res **35**:425–441, 1982.
7. Smeraglia R, Hochadel J, Varnell ED, Kaufman HE, Centifanto-Fitzgerald YM. The role of herpes simplex virus secreted glycoproteins in herpetic keratitis. Exp Eye Res **35**:443–459, 1982.
8. Whitley RJ, Alford CA, Hirsch MS, Schooley RT, Luby JP, Aoki FY, Hanley D, Nahmias AJ, Soong S-J, The NIAID Collaborative Antiviral Study Group. Herpes simplex encephalitis: adenine arabinoside versus acyclovir therapy. N Engl J Med **314**:144–149, 1986.
9. Landry ML, Berkovits N, Summers WP, Booss J, Hsiung GD, Summers WC. Herpes simplex encephalitis: Analysis of a cluster of cases by restriction endonuclease mapping of virus isolates. Neurology **33**:831–835, 1983.
10. Wander AH, Centifanto YM, Kaufman HE. Strain specificity of clinical isolates of herpes simplex virus. Arch Ophthalmol **98**:1458–1461, 1980.
11. Centifanto-Fitzgerald YM, Yamaguchi T, Kaufman HE, Tognon M, Roizman B. Ocular disease pattern induced by herpes simplex virus is genetically determined by a specific region of viral DNA. J Exp Med **155**:475–489, 1982.
12. Goodpasture EW, Teague O. Transmission of the virus of herpes febrillis along nerves in experimentally infected rabbits. J Med Res **44**:139–184, 1923.
13. Baringer JR, Swoveland P. Recovery of herpes simplex virus from human trigeminal ganglia. N Engl J Med **228**:648–650, 1973.
14. Stevens JG, Nesburn AB, Cook ML. Latent herpes simplex virus from trigeminal ganglia of rabbits with recurrent eye infection. Nature **235**:216–217, 1972.
15. Dinn JJ. Transolfactory spread of virus in herpes simplex encephalitis. Br Med J **281**:1392, 1980.
16. Griffith JF, Kibrick S, Dodge PR, Richardson EP. Experimental herpes simplex encephalitis. Electroencephalographic, clinical, virologic, and pathologic observations in the rabbit. Electroencephalogr Clin Neurophysiol **23**:263–269, 1967.
17. Anderson JR, Field HJ. The distribution of herpes simplex type 1 antigen in mouse central nervous system after different routes of inoculation. J Neurol Sci **60**:181–195, 1983.
18. Baringer JR. Herpes simplex virus infection of nervous tissue in animals and man. Prog Med Virol **20**:1–26, 1975.
19. Roizman B. Herpes simplex virus. In: Tooze J, Ed. DNA Tumor Viruses. Chap. 12. New York: Cold Spring Harbor Laboratories, 1980.
20. Centifanto-Fitzgerald YM. Initial herpes simplex virus type 1 infection prevents ganglionic superinfection by other strains. Infect Immun **35**:1125–1132, 1982.
21. Nesburn AB, Dunkel EC, Trousdale MD. Enhanced HSV recovery from neuronal tissues of latently infected rabbits. Pro Soc Exp Biol Med **162**:398–401, 1980.
22. Buchman TG, Simpson T, Nosal C, Roizman B, Nahmias AJ. The structure of herpes simplex virus DNA and its application to molecular epidemiology. In: Palese P, Roizman B, Eds. Genetic variation of viruses. New York: New York Academy of Sciences, Vol. **354**: pp279–290, 1980.
23. Lonsdale DM, Brown SM, Lang J, Subat-Sharpe JH, Koprowski H, Warren KG. Variations in herpes simplex virus isolated from human ganglia and a study of clonal variation in HSV-1. In: Palese P, Roizman B, Eds. Genetic variation of viruses. New York: New York Academy of Sciences. Vol. **354**: pp291–308, 1980.
24. Read SG, Person S, Keller PM. Genetic studies of cell fusion induced by herpes simplex virus type 1. J Virol **35**:105–113, 1980.
25. Ruyechan WT, Morse LS, Knipe DM, Roizman B. Molecular genetics of herpes simplex virus. II. Mapping of the major viral glycoproteins and of the genetic loci specifying the social behavior of infected cells. J Virol **29**:677–697, 1979.
26. Maclean AR, Brown M. Deletion and duplication variants around the long repeats of herpes simplex virus type 1 strain 17. J Gen Virol **68**:3019–3031, 1987.
27. Locker H, Frenkel N. BamI, KpnI, and SalI restriction enzyme maps of the DNAs of herpes simplex virus strains Justin and F: occurrence of heterogeneities in defined regions of the viral DNA. J Virol **32**:429–441, 1979.
28. Davison AJ, Wilkie NM. Nucleotide sequences of the joint between the L and S segments of herpes simplex virus types 1 and 2. J Gen Virol **55**:315–331, 1981.
29. Kaerner HC, Schroder CH, Ott-Hartmann A, Kumel G, Kirchner H. Genetic variability of herpes simplex virus: Development of a pathogenic variant during passaging of a nonpathogenic herpes simplex virus type 1 virus strain in mouse brain. J Virol **46**:83–93, 1983.
30. Javier RT, Thompson RL, Stevens JG. Genetic and biological analysis of herpes simplex virus enterty pic recombinant reduced specifically for neurovirulence. J Virol **61**:1978–1984, 1987.
31. Thompson RL, Cook ML, Devi-Roo GB, Wagner EK, Stevens JG. Functional and molecular analysis of the avirulent Weld-type herpes simplex virus type 1 strain KOS. J Virol **58**:203–211, 1986.
32. Sedarati F, Stevens JG. Biological basis for virulence of three strains of herpes simplex virus type 1. J Gen Virol **68**:2389–2395, 1987.
33. Becker Y, Hadar J, Tabor E, Ben-Hur, T, Raibstein I, Rosen A, Gholameraza D. A sequence in Hpa I-P fragment of herpes simplex virus-1 DNA determines intraperitoneal virulence in mice. Virology **149**:255–259, 1986.
34. Thompson RL, Stevens JG. Biological characterization of a herpes simplex virus intertypic recombinant which is completely and specifically non-neurovirulent. Virology **131**:171–179, 1983.
35. Thompson RL, Wagner EK, Stevens JG. Physical location of a herpes simplex virus type 1 gene function(s) specifically associated with a 10 million-fold increase in HSV-virulence. Virology **131**:180–192, 1983.